Supplementary Information

Pre-ciliated tubal epithelial cells are prone to initiation of high-grade serous ovarian carcinoma

Flesken-Nikitin et al.

Supplementary Figures

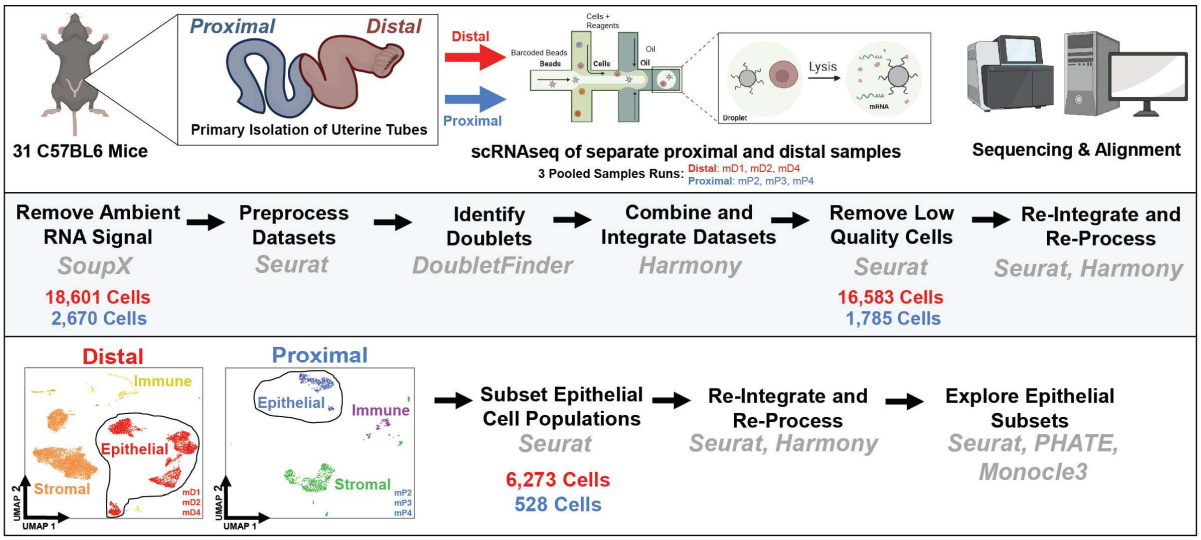

Supplementary Figure 1. Sample preparation and preprocessing. After isolation, separation, and dissociation of uterine tubes to single cell suspensions, the RNA from each cell was sequenced and processed *in silico* to make conclusions of the cell states present within the murine uterine tube. The epithelial subsets were created using the circled clusters from either the distal or proximal dataset. Figure was in part created with BioRender.com released under a Creative Commons Attribution-NonCommercial-NoDerivs license.

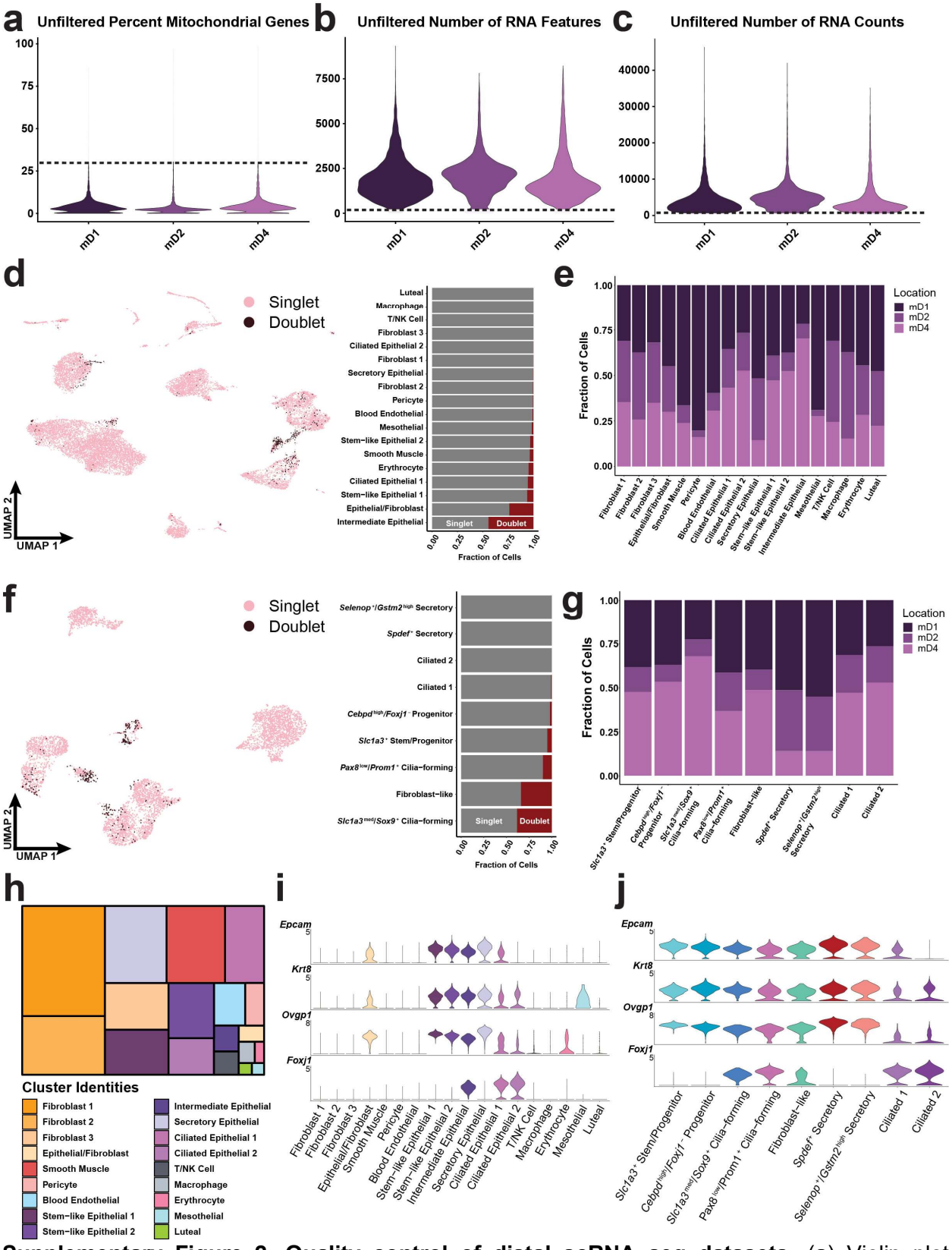

Supplementary Figure 2. Quality control of distal scRNA seq datasets. (**a**) Violin plot demonstrating mitochondrial gene percentage among different sample collection batches (mD1,

mD2, and mD4) with a cutoff of greater than 30%. (**b**) Violin plot demonstrating unique RNA features detected in each cell among different sample collection batches with a cutoff of less than 200. (**c**) Violin plot demonstrating total RNA counts detected in each cell among different sample collection batches with a cutoff of less than 750. (**d**) Doublets detected among cell clusters identified within the complete distal uterine tube dataset. (**e**) Distribution of different sample collection batches attributing to each cluster from the total distal uterine tube dataset. (**f**) Doublets detected among cell clusters identified within the distal epithelial subset. (**g**) Distribution of different sample collection batches attributing to each cluster from the distal epithelial subset. (**h**) Tile mosaic visualization of the relative distribution of cell types present within the distal dataset. (**i** and **j**) Violin plots of epithelial markers (*Epcam* and *Krt8*), and secretory (*Ovgp1*) and ciliated (*Foxj1*) markers within all distal cells (i) and within the distal epithelial subset (j). Source data are provided as a Source Data file.

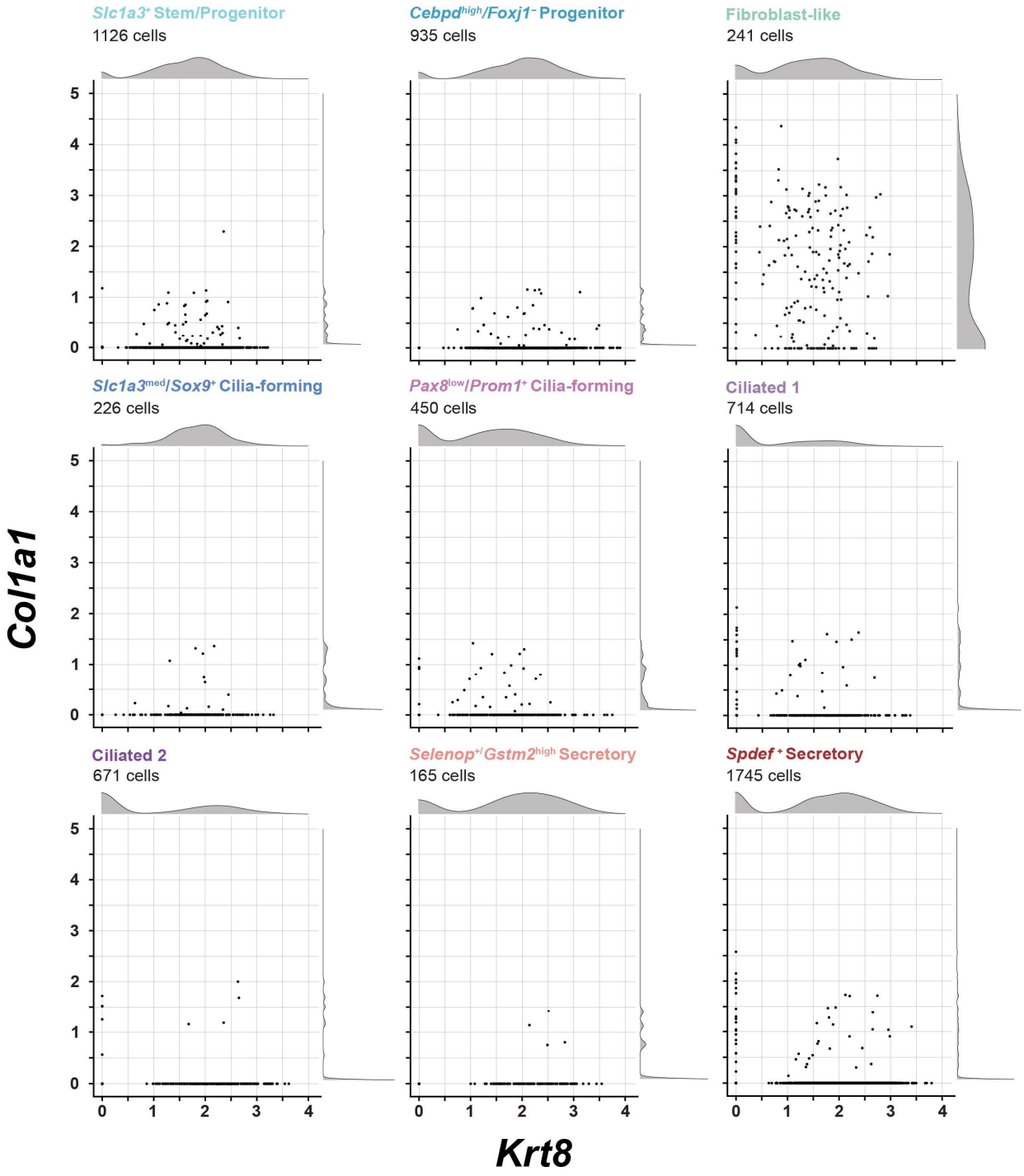

Supplementary Figure 3. Doublet detection of fibroblast and epithelial markers. Expression of fibroblast marker (*Col1a1*) and epithelial marker (*Krt8*) among epithelial subset clusters.

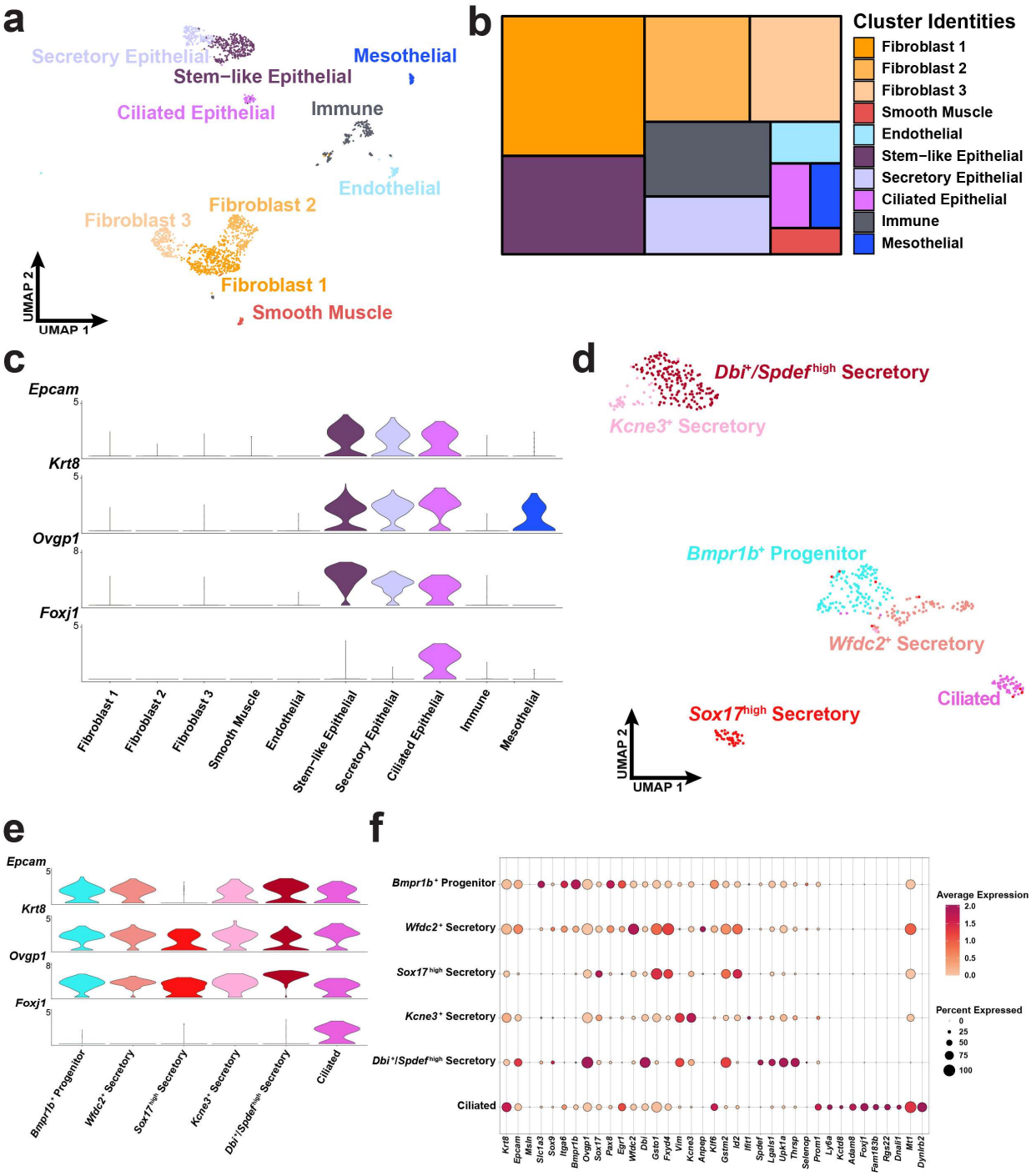

Supplementary Figure 4. Proximal uterine tube cell atlas. (**a**) Visualization of 1,785 high quality proximal cells from 62 uterine tubes within a UMAP embedding. (**b**) Tile mosaic visualization of the relative distribution of cell types present within the proximal dataset. (**c**) Violin plots of epithelial markers (*Epcam* and *Krt8*), and secretory (*Ovgp1*) and ciliated (*Foxj1*) markers within all proximal cells. (**d**) Epithelial cells were identified by their *Epcam* and *Krt8* expression and a subset of the remaining 528 epithelial cells were represented within the UMAP. (**e**) Violin plots of epithelial markers (*Epcam* and *Krt8*), and secretory (*Ovgp1*) and ciliated (*Foxj1*) markers

within all epithelial proximal cells. (**f**) Dot plot representation of genes associated with the proximal epithelial cells to justify cell state identification. Source data are provided as a Source Data file.

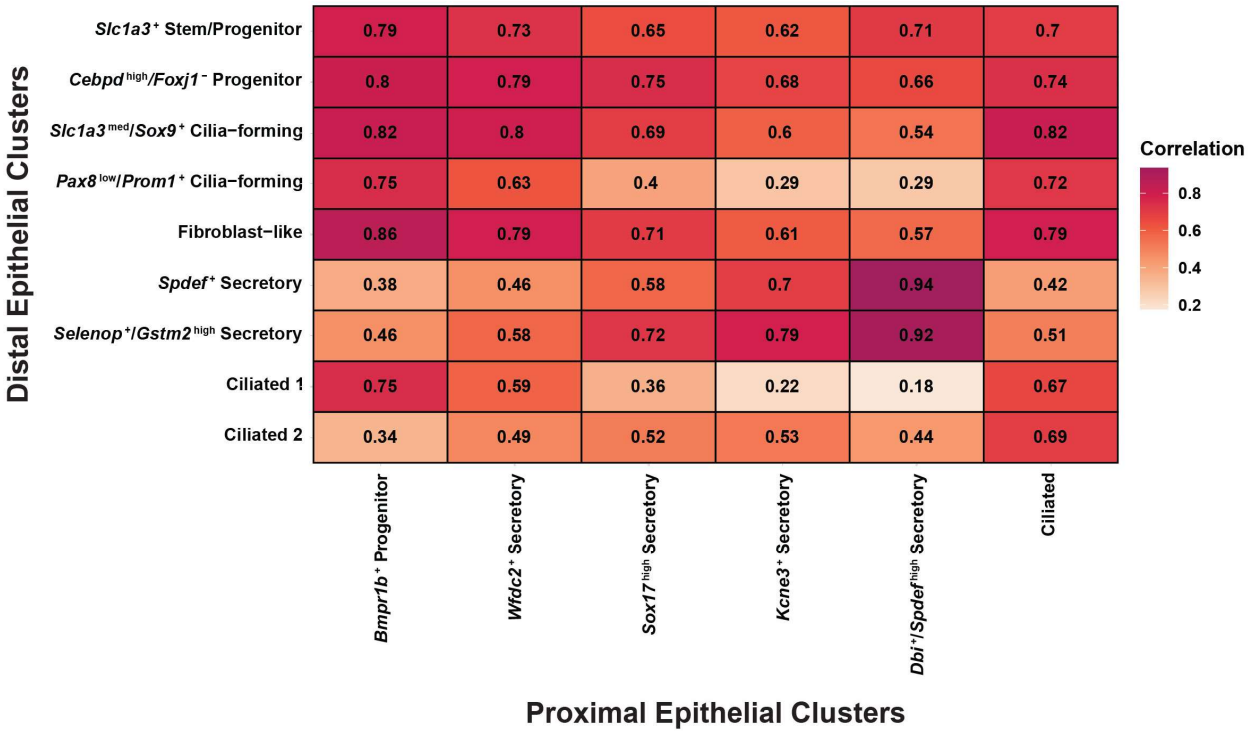

Supplementary Figure 5. Distal and proximal epithelial cell correlation. Correlation matrix comparing the average expression profiles of the distal and proximal epithelial clusters.

Supplementary Figure 6. General stem cell marker expression in epithelial cells. Markers associated with stemness were compiled and used to investigate which epithelial cell clusters may be stem-like. Source data are provided as a Source Data file.

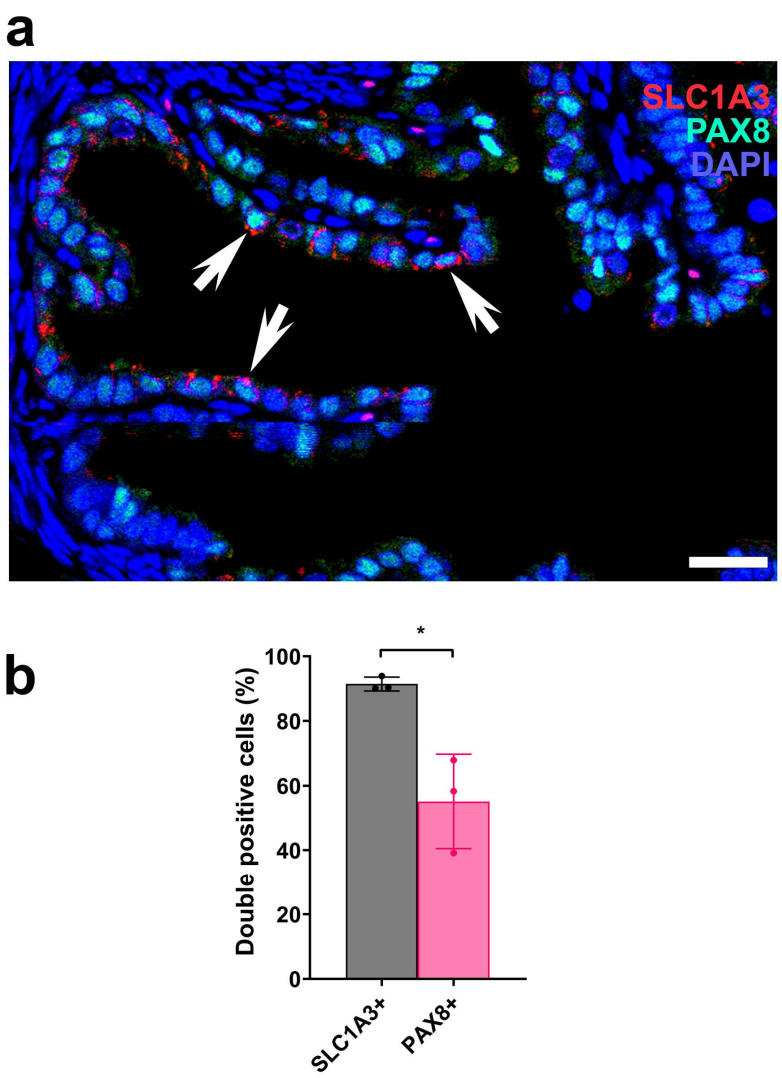

Supplementary Figure 7. PAX8 labels subset of SLC1A3+ cells. (**a**) SLC1A3+ cells (red) a contained for nuclear PAX8 (green), in the distal region of the uterine tube. Arrows indicate cells co-expressing PAX8 and SLC1A3. Counterstaining with DAPI. Scale bar represents 20 μm for all images. (**b**) Frequency of SLC1A3 expression in PAX8+ cells (SLC1A3+) and PAX8 expression in SLC1A3+ cells (PAX8+). *P=0.0131, two-tailed unpaired t-test. Data are presented as mean values +/- SD. Biological replicates (12 week-old mice) n=3 in each group (a and b). Source data are provided as a Source Data file.

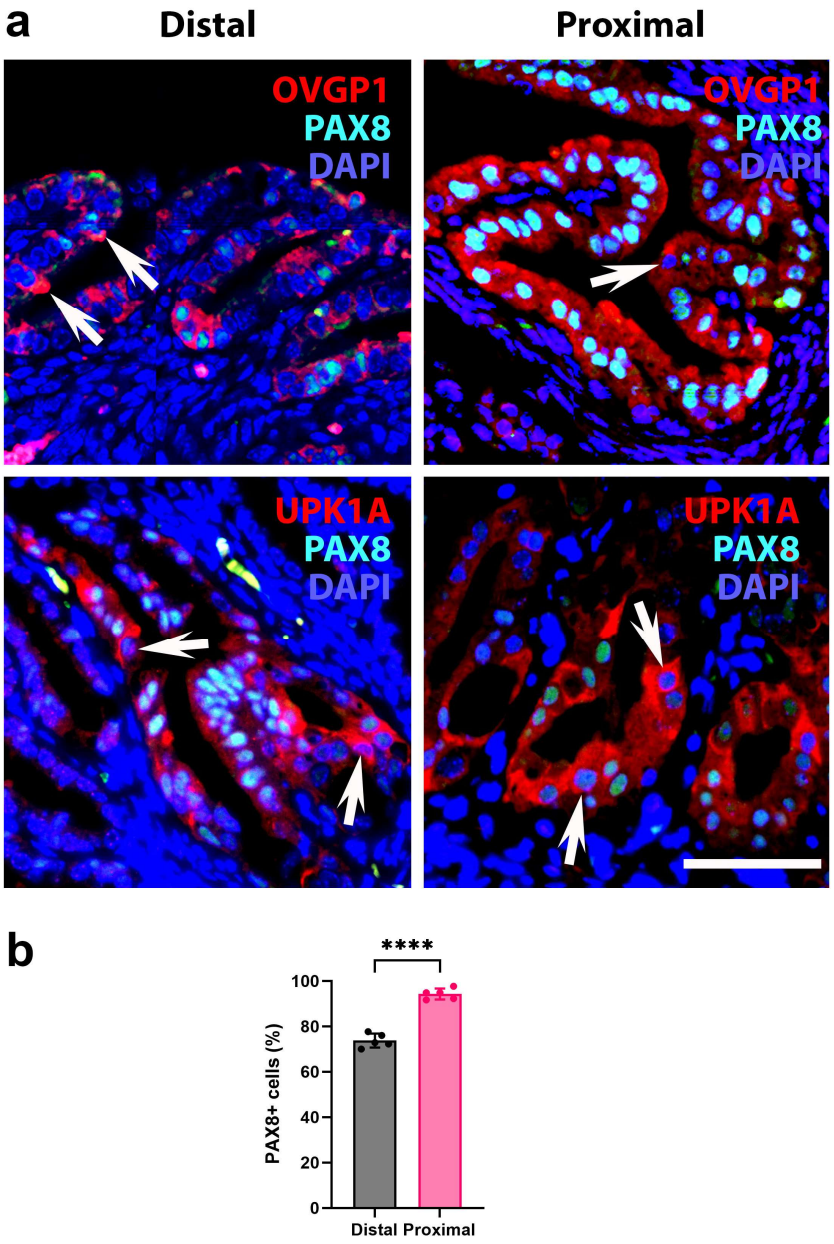

Supplementary Figure 8. Expression of PAX8 in secretory cells. (**a**) Secretory cells are detected by markers OVGP1 and UPK1A in both distal and proximal regions of the uterine tube. Arrows indicate secretory cells without detectable PAX8 expression. Counterstaining with DAPI. Scale bar represents 50 µm for all images. (**b**) Frequency of PAX8+ expression in OVGP1+ cells. Biological replicates (12 week-old mice) n=5 in each group (a and b). ****P < 0.0001 two-tailed unpaired t-test. Data are presented as mean values +/- SD. Source data are provided as a Source Data file.

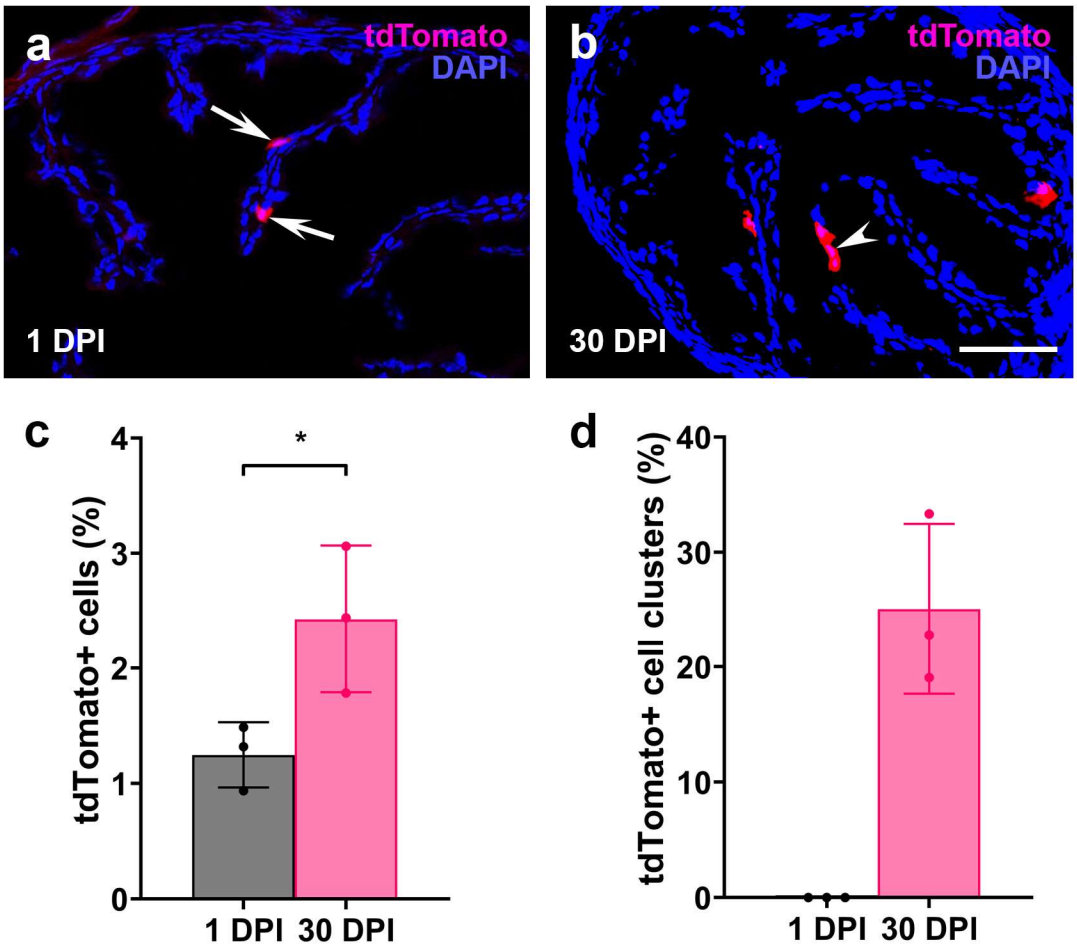

Supplementary Figure 9. Tracing fate of *Slc1a3*+ stem/progenitor cells after administration of a single low dose (10 µg/bw) of tamoxifen. (**a** and **b**) tdTomato expression (red) 1 (a) and 30 (b) days after injection (DPI) of tamoxifen. Counterstaining with DAPI. Arrows in a indicate single tdTomato+ cells. Arrowhead indicates 3 cell tdTomato+ cluster. Scale bar represents 50 µm for both images. (**c**) Quantification of cells expressing tdTomato in the distal region of the uterine tube 1 and 30 DPI. (**d**) Frequency of clusters containing ≥ 2 adjacent tdTomato+ cells. *P= 0.043, two-tailed unpaired t-test. No clusters were observed at 1 DPI. Data are presented as mean values +/- SD. Biological replicates n=3 in each group (a-d). Source data are provided as a Source Data file.

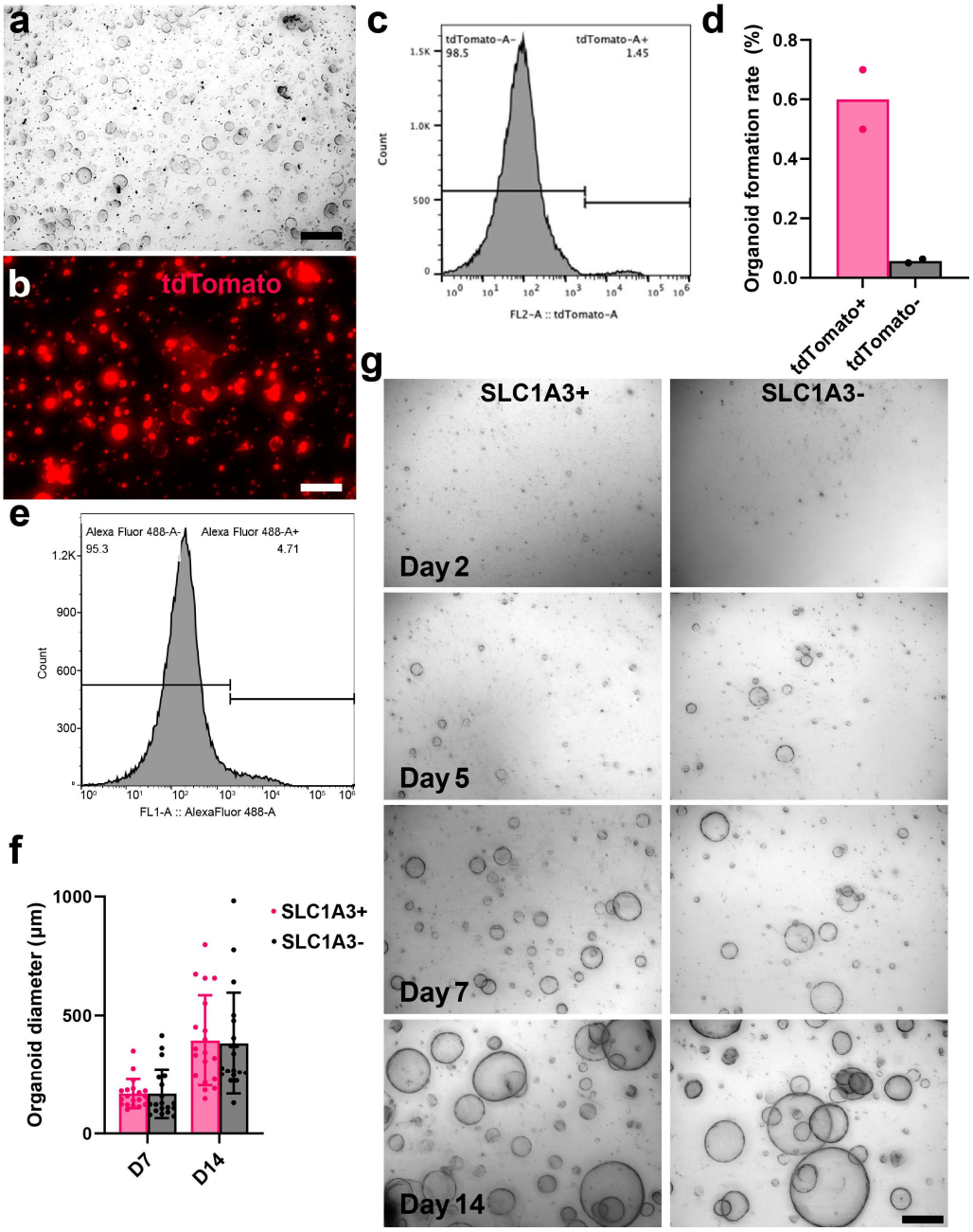

Supplementary Figure 10. Tubal epithelium (TE) organoid formation. (**a-b**) Organoid formation by distal TE cells isolated from Slc1a3-CreERT Ai9 mice and treated with tamoxifen. Phase contrast (a) and tdTomato fluorescence (red, b). (**c**) Representative histogram of tdTomato+ TE cells separated by FACS 36 hours after tamoxifen administration. (**d**) Quantification of organoid formation rate of TE cells separated for tdTomato expression by FACS. Biological replicates n=2. (**e**) Representative histogram of SLC1A3+ TE cells separated by MACS. (**f**) Organoid size measured 7 days and 14 days between SLC1A3+ and SLC1A3- cells from two MACS experiments (n=19). (**g**) Representative images of SLC1A3+ and SLC1A3- organoids 2, 5, 7, and 14 days after isolation from a single MACS experiment. Scale bar represents 170 µm (a and b) and 500 µm (g). Source data are provided as a Source Data file.

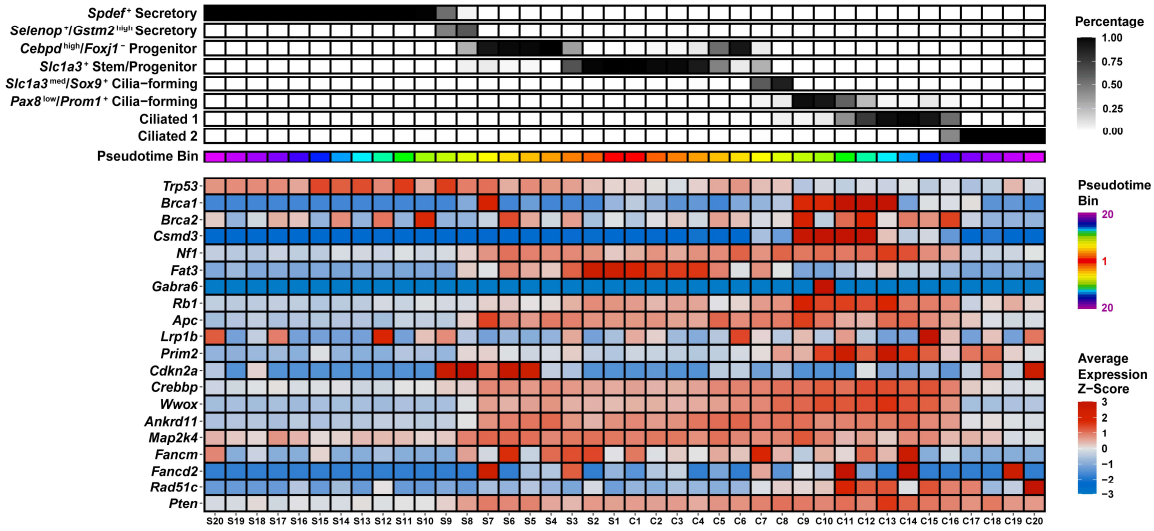

Supplementary Figure 11. Expression of putative HGSC driver genes along inferred pseudotime trajectories of secretory and ciliated epithelial cell lineages. The average z-scored expression was calculated for each gene. Each pseudotime bin is equally sized and consists of about 150 cells. Driver genes were derived from the Cancer Genome Atlas Research Network. Most genes, except for FANCM and APC were found to be significantly mutated or deleted in HGSC tumors by TCGA[1, 2]. Source data are provided as a Source Data file.

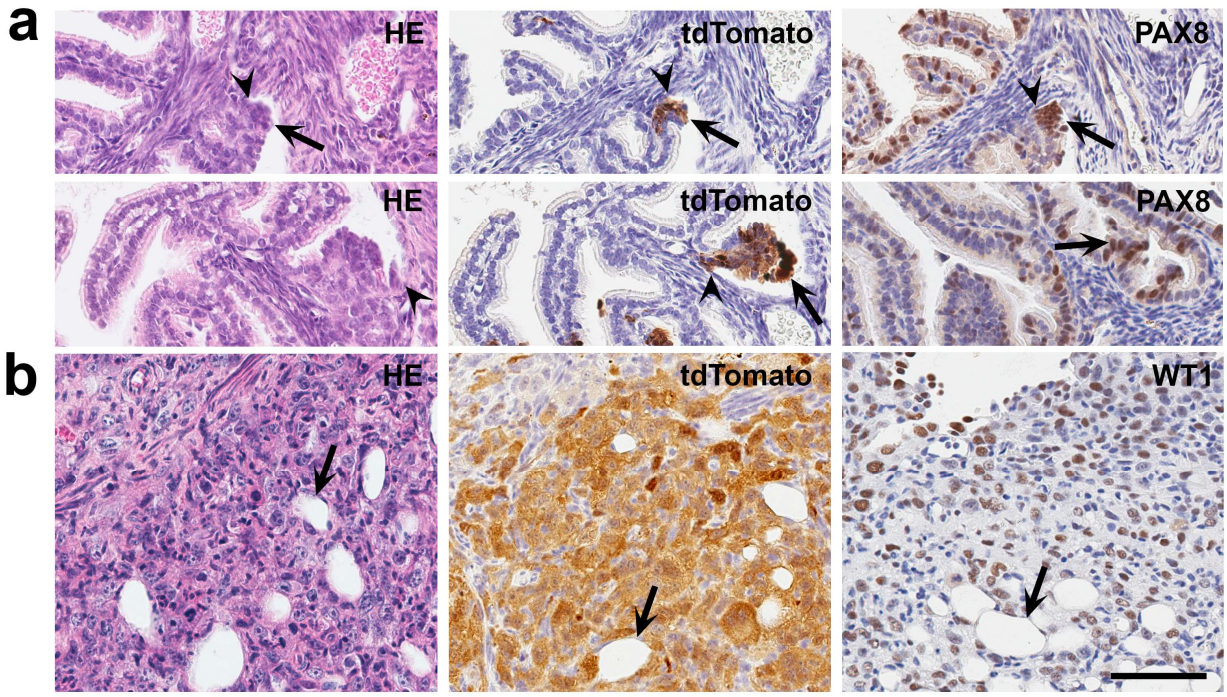

Supplementary Figure 12. Neoplastic lesions in Krt5-CreERT *Trp53*$^{loxP/loxP}$ *Rb1*$^{loxP/loxP}$ Ai9 mice. (**a**) Early lesions (arrows) located at TE-mesothelial junctions. (b) Invasion of ovarian fat pad (arrows). Hematoxylin and Eosin (HE) staining and immunostaining for tdTomato, PAX8 and Wilms Tumor 1 (WT1). Elite ABC method, hematoxylin counterstaining. Scale bar, 60 μm for all images. Biological replicates n=5 (a) and n=3 (b).

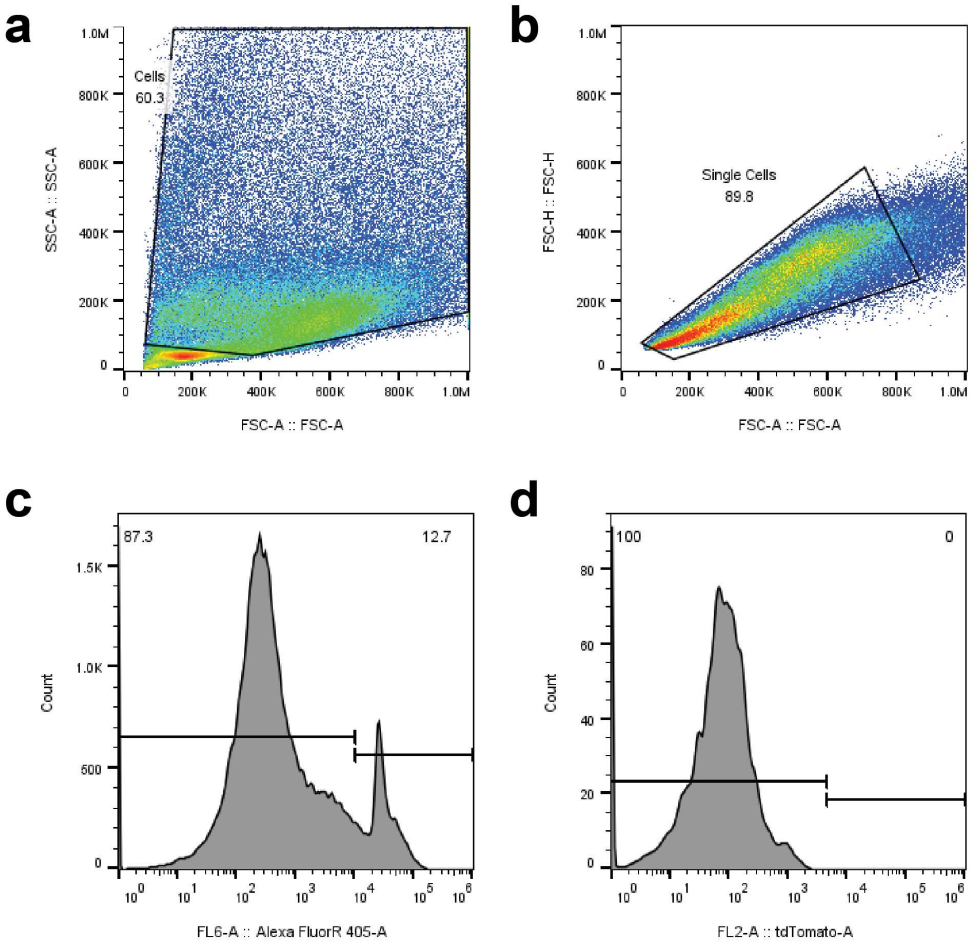

Supplementary Figure 13. Gating strategy for tdTomato+ TE cells. (**a**) Forward scatter (FSC) and side scatter (SSC) gating strategy for removal of debris within distal TE cells isolated from Slc1a3-CreERT Ai9 mice after tamoxifen treatment. (**b**) FSC gating for single cell purification. (**c**) SYTOX Blue dead cell staining to remove positively stained dead cells. (**d**) Counts for tdTomato+ distal TE cells isolated from Ai9H mice after tamoxifen treatment as a negative control.

Supplementary Table 1.
Frequency of cell types in the uterine tube

Cell States	Total Cells		Total *Pax8*+ Cells	
	N	% of Total	N	% of Total
Distal Tubal Epithelium				
Individual Clusters				
Ciliated 1	714	11.38	20	2.80
Ciliated 2	671	10.70	26	3.87
*Pax8*low/*Prom1*+ Cilia-forming	450	7.17	168	37.33
*Slc1a3*med/*Sox9*+ Cilia-forming	226	3.60	163	72.12
Slc1a3+ Stem/Progenitor	1126	17.95	917	81.44
*Cebpd*high/*Dbi*+ Progenitor	935	14.91	602	64.39
Selenop+/*Gstm2*high Secretory	165	2.63	35	21.21
Spdef+ Secretory	1745	27.82	492	28.19
Fibroblast-like	241	3.84	158	65.56
Total	6273	100	2581	41.14
Cell Type Groupings				
All ciliated and cilia forming cells	2061	32.86	377	18.29
All secretory cells	1910	30.45	527	27.59
Slc1a3+ Stem/Progenitor cells	1126	17.95	917	81.44
Transitional cilia-forming cells	676	10.78	331	48.96
Proximal Tubal Epithelium				
Individual Clusters				
Ciliated	55	10.42	16	29.09
Bmp1rb+ Progenitor	130	24.62	88	67.69
Wfdc2+ Secretory	80	15.15	49	61.25
*Sox17*high Secretory	50	9.47	11	22.00
Kcne3+ Secretory	41	7.77	6	14.63
Dbi+/*Spdef*high Secretory	172	32.58	35	20.35
Total	528	100	205	38.83
Cell Type Groupings				
All ciliated and cilia forming cells	55	10.42	16	29.09
All secretory cells	343	64.96	101	29.45
Progenitor cells	130	24.62	88	67.69

Supplementary Table 2.
Impact of tamoxifen administration on frequency of SLC1A3+ cells

Compound	Tamoxifen	Oil
1 DPI[#]	18.07 ± 5.63	19.00 ± 4.29
30 DPI	18.04 ± 5.36	17.89 ± 2.81

*Oil administration instead of Tamoxifen
[#] DPI, days post injection
Mean ± s.d., n=3 for tamoxifen 1 DPI and Oil 1 and 30 DPI, n=4 for tamoxifen 30 DPI.

Supplementary Table 3.
Magnetic-activated cell sorting (MACS) for organoid-forming SLC1A3+ and SLC1A3- cells.

Fractions*	Total cells (± s.d.)	Fraction of total cells (%)
After primary isolation	$5.66x10^5 \pm 1.47x10^5$	100
After stromal removal	$2.76x10^5 \pm 0.65x10^5$	48.8
SLC1A3+ cells	$0.20x10^5 \pm 0.13x10^5$	3.5
SLC1A3- cells	$2.55x10^5 \pm 0.49x10^5$	45.1

*Total cells and percentages were determined by cell counts made from cell fractions at different stages of MACS preparation.

Supplementary Table 4.
Neoplastic TE lesions after Cre-*LoxP* mediated inactivation of *Trp53* and *Rb1*

Promoter	*Slc1a3*	*Pax8*	*Krt5*
Cases, N	19	21	21
First detection (DPI)	NA*	154	104
End point (DPI)	360	400	200
Targeted cells (%)[#]	11.91±3.23	18.89±5.66	0.83±0.49
Mice with TE lesions (%)	0	58.33	76.00

*NA, no applicable, no lesions detected
[#] According to tdTomato detection in Ai9 mice crossed to "Cre" mice
Mean ± SD, n=6 for *Slc1a3,* n=4 for *Pax8* and *Krt5* each. *Pax8 vs Krt5* two-tailed unpaired t test P=0.0007.

Supplementary Table 5.
Quantification of cells expressing tdTomato in the distal TE and OSE of Krt5-CreERT Ai9 mice at 1 and 30 DPI.

Epithelium	TE		OSE	
DPI	1	30	1	30
Labeled cells (%)*	0.83±0.49	4.29±1.64	0.20±0.04	0.14±0.02
N	4	3	4	4

*Mean ± SD,
Two-tailed unpaired t tests:
TE 1 DPI vs TE 30 DPI P=0.0094, OSE 1 DPI vs OSE 30 DPI P=0.031
TE 1 DPI vs OSE, 1 DPI P=0.0426, TE 30 DPI vs OSE 30 DPI P=0.003

Supplementary Table 6.
List of genotyping primers.

Mouse strain*	Gene detected	Primer name	Sequence (5' → 3')	PCR products
Rosa-loxP-stop-loxP-tdTomato/Ai9	Ai9	Ai9-1	AAGGGAGCTGCAGTGGAGTA	297bp-Wild type
		Ai9-2	CCGAAAATCTGTGGGAAGTC	196bp-Mutant
		Ai9-3	GGCATTAAAGCAGCGTATCC	
		Ai9-4	CTGTTCCTGTACGGCATGG	
K5-Cre-ERT2	*Cre*	Cre5'	GGACATGTTCAGGGATCGCCAGGC	269bp-Mutant
		Cre3'	GCATAACCAGTGAAACAGCATTGCT	
Pax8-rtTA	*rtTA*	F-rtTA	GGTATCGAAGGCCTGACGACAAGGAA	324bp-Wild type
		R-rtTA	AGTCTTGCCATGACTCGCCTTCCA	172bp-Mutant
		F-con	CTAGGCCACAGAATTGAAAGATCT	
		R-con	GTAGGTGGAAATTCTAGCATCATCC	
Rb1$^{loxP/loxP}$	*Rb1*	Rb212	CGAAAGGAAAGTCAGGGACATTGGG	295bp-Floxed
		Rb183'	GGAATTCCGGCGTGTGCCATCAATG	247bp-Wild type
		Rb19E	AGCTCTCAAGAGCTCAGACTCATGG	269bp-Knockout
Slc1a3-CreERT	*Slc1a3*	10112	ACAATCTGGCCTGCTACCAAAGC	200bp-Wild type
		10110	CCAGTGAAACAGCATTGCTGTC	600bp-Mutant
		F-8744	CAAATGTTGCTTGTCTGGTG	
		R-8745	GTCAGTCGAGTGCA AGTTT	
Tre-Cre	*Cre*	Cre5'	GGACATGTTCAGGGATCGCCAGGC	269bp-Mutant
		Cre3'	GCATAACCAGTGAAACAGCATTGCT	
Trp53$^{loxP/loxP}$	*Trp53*	P531F5'	GTGCCCTCCGTCCTTTTTCGCAATC	316bp-Floxed
		P5310F5'	GTTAAGGGGTATGAGGGACAAGGTA	163bp-Wild type
		P53102.3'	CCATGAGACAGGGTCTTGCTATTGT	198bp-Knockout

*See Methods for strain descriptions.

Supplementary Table 7.
List of antibodies used for immunostaining*

Antigen, conjugation	Antibody source, catalogue number	Clone	Lot. number	Host	Retrieval	Dilution
Acetylated α-tubulin	Sigma-Aldrich, T7451	6-11B-1	103M4772V	Mouse	Citrate	1:200 (IF[#])
CD140a	Biolegend, 135910	APA5	B376160	Rat		(MACS[$])
CD31	Biolegend, 102503	MEC13.3	B379519	Rat		(MACS)
CD45	Biolegend, 103103	30-F11	B394828	Rat		(MACS)
FAM183B	Invitrogen, PA5-71109	PC[&]	ZE4342976	Rabbit		1:150 (IF)
FOXJ1	Novus Biologicals, AF3619-SP	PC	XVG022308	Goat		1:800 (IF)
Ki67	Thermo Fisher, 14-5698-82	SolA-15	2496198	Rat	Citrate	1:4000 (IHC[†])
OVGP1	Abcam, Ab118590	PC	1078217-2	Rabbit	None Citrate	1:600 (IF) 1:2000-8000 (IHC), 1:800 (IF)
P16	Abcam, Ab241543	PABLO-33B	-	Rat	Citrate	1:500 (IHC)
P73	Abcam, Ab40658	EP436Y	1014031-3	Rabbit	Citrate	1:200 (IF)
PAX8	Proteintech, 60145-4-Ig	4H7B3	10003229	Mouse	Citrate	1:5000-10000 (IHC), 1:100 (IF)
PAX8	Proteintech, 10336-1-AP	PC	-	Rabbit	Citrate	1:4000 (IHC), 1:400 (IF)
RFP/tdTomato	Rockland Immunochemical, 200-101-379	PC	50005	Goat		1:100 (IF)
RFP/tdTomato	Rockland Immunochemical, 600-401-379S	PC	48776	Rabbit		1:4000 (IHC), 1:250 (IF)
SLC1A3	Novus Biologicals, NB100-1869	PC	D112656-5	Rabbit		1:1000 (IHC), 1:500 (IF)
SLC1A3/ EAAT1	R&D Systems, AF6048	PC	CAGI032408A	Sheep	Citrate	1:75 (IF)
SLC1A3	Novus Biologicals, NB-100-1869B	PC	D160350	Rabbit		(MACS)
TER-119	Biolegend, 116203	TER-119	B378223	Rat		(MACS)

UPK1α	Proteintech, 25275-1-AP	PC	-	Rabbit	Citrate	1:4000 (IHC), 1:250 (IF)
Wilm's Tumor Protein 1	Abcam, Ab267377	EPR-23963	-	Rabbit	Citrate	1:500 (IHC)
Anti-goat IgG, Alexa Fluor 594	Invitrogen, A11058	PC	2185074	Donkey		1:200
Anti-mouse IgG, biotinylated	Vector Labs, BA-9200-1.5	PC	ZH0819	Goat		1:200
Anti-mouse IgG, Alexa Fluor 488	Thermo Fisher, A-11001	PC	2714439	Goat		1:200
Anti-rabbit IgG, biotinylated	Vector Labs, BA-1000-1.5	PC	ZG0122	Goat		1:200
Anti-rabbit IgG, Alexa Fluor 488	Invitrogen, A21206	PC	2072687	Donkey		1:200
Anti-rabbit IgG, Alexa Fluor 594	Thermo Fisher, A-21207	PC	2747441	Donkey		1:200
Anti-rat IgG, biotinylated	Vector Labs, BA-4000-1.5	PC	ZJ1101	Rabbit		1:200
Anti-sheep IgG, Alexa Fluor 594	Invitrogen, A11016	PC	2260924	Donkey		1:200

*All antibodies were validated by manufacturers.
[#]IF, Immunofluorescence
[$]MACS, Magnetic activated cell sorting, all dilutions were 0.5 µg of antibody per million cells
[&]PC: Polyclonal
[†]IHC, Immunohistochemistry (ABC Elite method)

Supplementary References

1 Yamulla, R. J., Nalubola, S., Flesken-Nikitin, A., Nikitin, A. Y. & Schimenti, J. C. Most Commonly Mutated Genes in High-Grade Serous Ovarian Carcinoma Are Nonessential for Ovarian Surface Epithelial Stem Cell Transformation. *Cell Rep* **32**, 108086 (2020). https://doi.org/10.1016/j.celrep.2020.108086

2 Network, T. C. G. A. R. Integrated genomic analyses of ovarian carcinoma. *Nature* **474**, 609-615 (2011). https://doi.org/10.1038/nature10166